International Journal of Scientific Research in Engineering and Management (IJSREM)
Volume: 09 Issue: 12 | Dec - 2025 SJIF Rating: 8.586 ISSN: 2582-3930

Crashworthiness Analysis of Thin Tubular Sections

Shoaib Akhtar[1*], Mohd. Areeb[1], Danish Iqbal[1]

[1]*Department of mechanical engineering, Aligarh Muslim University, Uttar Pradesh, India*

---***---

Abstract - This study presents a numerical investigation into the influence of geometric discontinuities on the energy absorption and crushing response of thin-walled aluminium square sections. Four configurations are examined: a solid tube (no hole), tubes with two circular holes, elliptical holes, and corner holes. All discontinuities are introduced 30 mm from the top, with an equal percentage of material removal maintained across the perforated cases.

The tubes are subjected to gradual axial and oblique loading at 0°, 30°, and 45° to evaluate how discontinuity type and loading angle affect crashworthiness behaviour. The analysis highlights the role of crush angle and initial impact contact in initiating plastic collapse and shaping the subsequent deformation pattern.

Key crashworthiness indicators Energy Absorption (EA), Mean Crushing Force (MCF), Crush Load Efficiency (CLE), and Specific Energy Absorbed (SEA) are computed to assess performance across configurations. The results provide insight into how different discontinuity shapes and orientations influence the collapse mechanism and overall energy absorption capability. These findings support the improved design of thin-walled aluminium energy absorbers for enhanced crashworthiness in practical applications.

Key Words: Crashworthiness; Thin-walled aluminium tubes; Geometric discontinuities; Energy absorption; Oblique loading; Finite element analysis.

1. INTRODUCTION

Crashworthiness is the ability of a structure to protect the occupants of the structure during an impact. Across the transportation industry, a new and challenging field of engineering analysis developed with the introduction of automobile safety rules during the early 1960s. Apart from the standard requirements, thin- walled these days, Structures are made to withstand unusual loadings that occur due to a variety of events. In the automotive industry, vehicle manufacturers are always in competition to create vehicles with better performance and a higher safety standard. As a result, the study of vehicle crashworthiness has become an important area of research, focused on providing occupant protection during collision events. Crashworthiness basically refers to a study of plastic deformation behavior of structural components under impact loading. Numerous studies have been done on critical energy absorbing structures such as vehicle frames, helicopter subfloors, and highway safety barriers. The basic goal of such studies would be to reduce the risk of fatal injuries to the occupants by enhancing the energy absorption capacities of the structures in case of unfortunate situations like an impact, crash and collision [1].

During a vehicle collision, the crash box can act as one of the primary energy-absorbing components by experiencing progressive plastic deformation, thus reducing the transmission of the impact loads to the structures of the vehicle located behind the crash box, increasing the safety of the occupant. In an ideal crash situation, the crash box is developed to be deformed before other structural members, absorbing maximum possible energy and thus reducing the repair costs after a crash. However, the increased interest in car lightweighting has led to the wide use of thin-walled metallic structures, which is a problem when it comes to achieving an adequate energy absorption capacity. Therefore, a detailed knowledge of the effect of material choice and geometric configuration on the deformation behavior is crucial for the design of crash boxes with stable modes of collapse and better energy absorption performance [2]. This crash box construction is anticipated to be able to absorb kinetic energy in frontal collisions, keep the vehicle's deceleration within acceptable bounds, and reduce the likelihood of passenger injuries during collisions as a passive safety system in a car [3]. Although it covers a wide range of topics and methods, the study of crash box construction primarily advances the subject of crashworthiness research. The crash box's design is one of the most talked-about. To comprehend their plastic deformation behaviour and how effectively they can adapt as an energy-absorbing component, several thin-wall structures, including cylindrical, square/polygonal, conical/tapered, and hat-sectional beams, have been studied and compared [2], [4].

Several researchers have investigated the impact of dimensions and thickness of thin-walled structures on crash performance [[4], [5], [6]]. Different designs of crash boxes with various parameters, including fillings [[7],[8]], hybrid, and multi-cell configurations have been evaluated [[4],[6]]. A study of imperfection configuration is conducted to examine the energy absorbed by the flawed thin-wall structure [[2]].

2. Material model

The tested Aluminium tube is made of A6060 alloys because of their good mechanical properties (Table 1),
subjected to impact load. To develop effective numerical models, A6060 play a significant role in modern engineering and manufacturing, owing to their lightweight nature, high strength-to-weight ratio, and corrosion resistance. Among these alloys, Aluminium 6060 stands out as a versatile material suitable for a wide range of applications. This paper aims to delve into the properties of aluminium 6060, shedding light on its composition, mechanical behaviour, thermal characteristics, and practical applications. It is crucial to precisely determine the constitutive model parameters of materials. One of the most popular constitutive models is the Johnson-Cook (J-C) model because to its straightforward but efficient operation. The following is an expression for this model: model parameters of materials. One of the most popular constitutive models is the Johnson-Cook (J-C) model because of its straightforward but efficient operation. The following is an expression for this model:

$$\sigma = (A + B\varepsilon^n)(1 + C ln\varepsilon^*)[1 - (\frac{T-T_r}{T_m-T_r})^m] \quad (1)$$

where σ is a stress, n is the strain hardening coefficient, B is the strain hardening constant, A is the material's yield stress under reference conditions, and ε is the strain, $\varepsilon*$ is the strain rate, C is the strain rate factor, and n and m are the work-hardening exponent and the thermal softening exponent, respectively., T, Tm, and Tr are the temperature, melting point and reference temperature (usually room temperature)

Table -1: Material properties table of Al6060

Description	Variable	Value
Density (kg/m3)	ρ	2700
Young modulus (GPa)	E	65.76
Poisson ratio (-)	u	0.3
Yield Stress (MPa)	A	148.361
Strain hardening constant (MPa)	B	345.513
Strain rate factor	C	0.001
Strain rate (s−1)	ε^*	0.0001
Melting temperature (K)	T_m	893
Reference temperature (K)	T_r	300
Work hardening exponent	n	0.183
Thermal softening exponent	m	0.859

3. Crashworthiness Response Parameters

The crashworthiness performance of the investigated tubes is tested by quantification of several known crashworthiness response measures. These metrics include energy absorption ability, plastic collapse initiation, and crushing efficiency. The first important parameter is total energy absorption (EA) which is transformed from crushing kinetic energy to plastic deformation energy during the plastic collapse and then wasted. Assuming that dx is the maximum displacement of the impacting body and F(x) is the instant crushing force, the area under the force displacement curve is determined as, EA equals to total area under the force displacement curve as shown below:

$$\text{EA}(dx) = \int x\ Fdx \qquad (2)$$

Another important parameter for the further analysis of energy absorber is the peak crushing force (PCF) and mean crushing force (MCF). The term PCF, which means “the maximum crushing force required to initiate plastic failure, while MCF is defined as the ratio of energy absorption to the maximum displacement of the impactor. Thus, both are expressed, respectively, as follows:

$$PCF = Max\{F(x)\} \qquad (3)$$

$$MCF = \frac{EA(dx)}{dx} \qquad (4)$$

However, On the other hand, specific energy absorption (SEA), which indicates the absorbed energy per unit mass of the crushed structure (m), is a more accurate measure for evaluating the energy- absorption capability of structures. Which is expressed as follows:

$$SEA = \frac{EA(dx)}{m} = \frac{EA(dx)}{\rho Ax} \qquad (5)$$

4. FEM Analysis

A numerical study of the crashworthiness response was performed using non-linear explicit dynamic finite element (FE) analysis using Abaqus software. A series of numerical simulations of the quasi-static axial and oblique crushing of the 5 types of tube samples were conducted i.e. (without holes, two holes, Corner hole and Elliptical Hole and all these at an angle of 0, 30 and 45 degrees.

For the FEA analysis purpose, we consider a thin-walled square tube of cross-section 50x50 mm and length of 200 mm considering all the cases. All the discontinuities are 30mm from the top. The proper finite element mesh density is generated in such a way that the shell thickness is 2 mm, as dimension, which is nearly identical to the thickness of the tube wall, will yield dependable outcomes regarding the fold formulation of slender-walled structures.

Thin-walled tested tubes are simulated using four-node shell elements (S4R), as their precision in forecasting the failure mechanism regarding the collapse mode and the count of developed folds has proven to be more dependable than alternatives for thin-walled constructions. In comparison, the impactor and bottom-holder base are represented by four-node solid elements (R3D4), as they consist of dense rigid bodies.

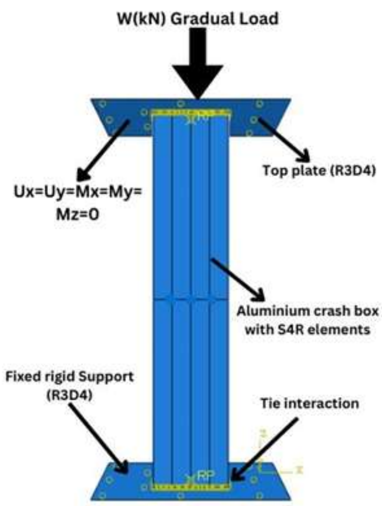

Fig -1: Boundary condition

4.1 Specimens

We considered four different types of specimens i.e, without hole, two holes, elliptical hole and corner holes, respectively. For this analysis we keep removed area almost constant in three cases.

Fig -2: Specimens

5. Simulation results

Figures (3-14), present the deformation patterns at representative crushing stages for all configurations under axial and oblique loading. The corresponding force–displacement curves are shown in Figures Z–W. These plots are used to discuss the influence of discontinuity type and crush angle on collapse initiation, peak load, post-buckling stability, and overall energy absorption.

5.1 At 0-degree angle

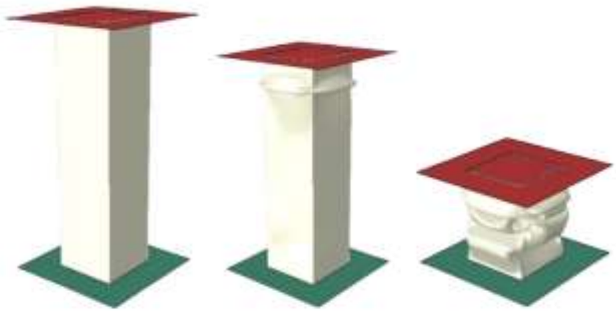

Fig -3: Deformation sequence of the intact tube under axial crushing (0°).

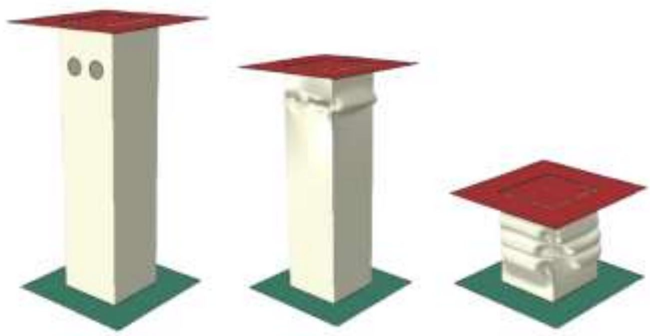

Fig -4: Deformation sequence of the two-hole tube under axial crushing (0°).

Fig -5: Deformation sequence of the elliptical-hole tube under axial crushing (0°).

Fig -6: Deformation sequence of the corner-hole tube under axial crushing (0°).

5.2. At an angle 30 degree.

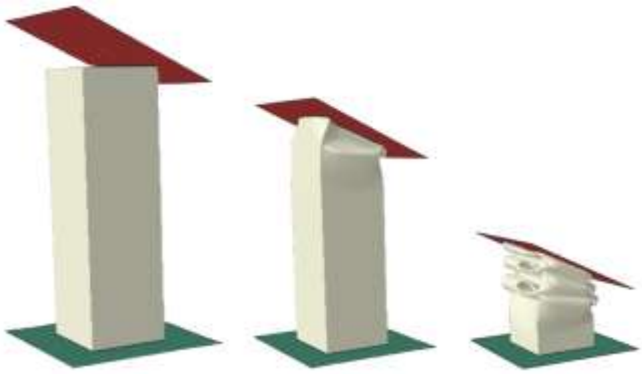

Fig -7: Deformation sequence of the intact tube under oblique crushing (30°).

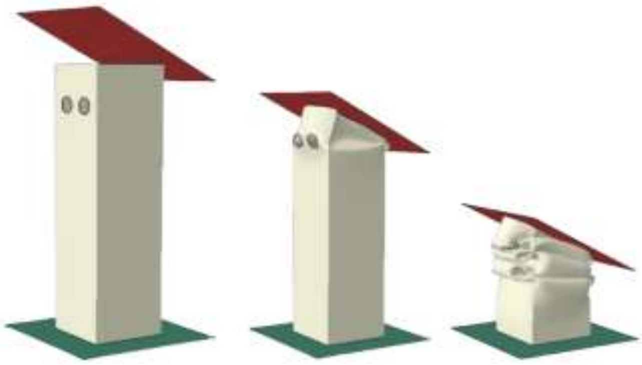

Fig -8: Deformation sequence of the two-hole tube under oblique crushing (30°).

Fig -9: Deformation sequence of the elliptical-hole tube under oblique crushing (30°).

Fig -10: Deformation sequence of the corner-hole tube under oblique crushing (30°).

5.3 At an angle 45 degree

Fig -11: Deformation sequence of the intact tube under oblique crushing (45°).

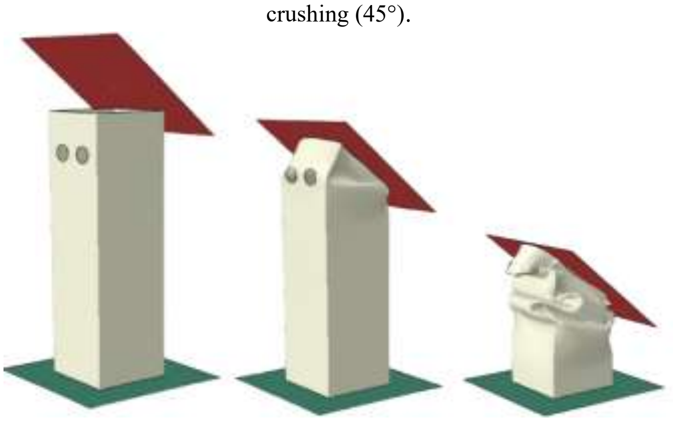

Fig -12: Deformation sequence of the two-hole tube under oblique crushing (45°).

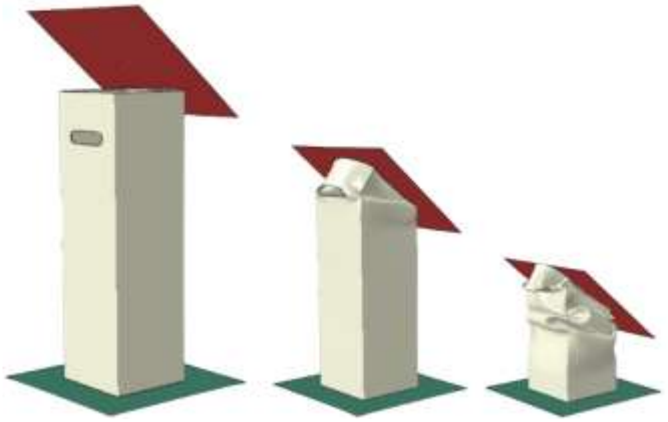

Fig -13: Deformation sequence of the elliptical-hole tube under oblique crushing (45°).

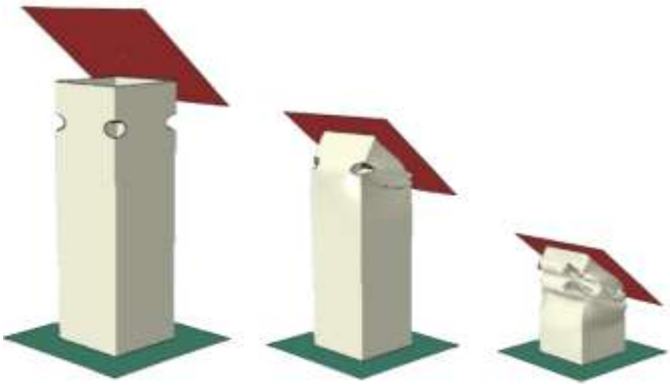

Fig -14: Deformation sequence of the corner-hole tube under oblique crushing (45°).

6. Graphs

Figures (15-17) present the **force–displacement responses** of the intact and perforated tubes under **0°, 30°, and 45°** crushing. The curves are used to identify the **peak crushing force (PCF)** at the onset of collapse and to evaluate the subsequent **progressive folding behavior**, which governs the **mean crushing force (MCF)** and the total **energy absorption (EA)** (area under the curve). In the axial case, the response is characterized by a distinct initial peak followed by a relatively stable post-buckling region, whereas under oblique loading the curves show reduced peak force and a more irregular force evolution due to the increased contribution of bending and asymmetric deformation. The comparison between configurations highlights how discontinuity geometry modifies collapse initiation and the stability of the post-peak crushing stage, which directly controls the crashworthiness indicators reported in the following sections.

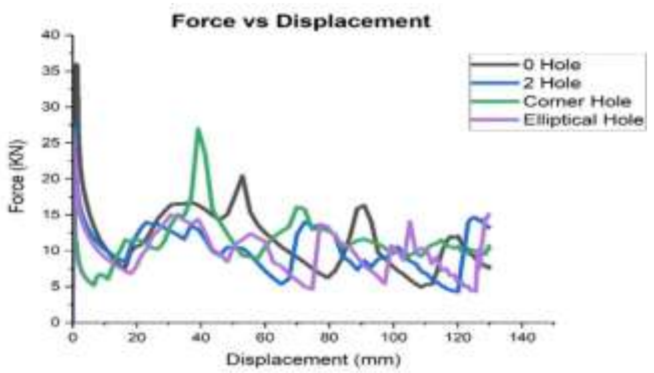

Fig -15: Force–displacement curves for all tube configurations at 0° (axial).

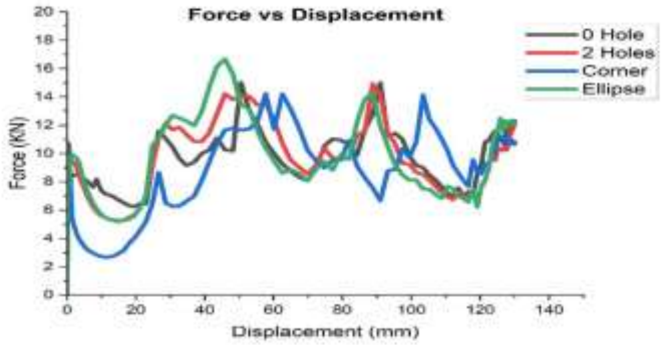

Fig -16: Force–displacement curves for all tube configurations at 30° (oblique).

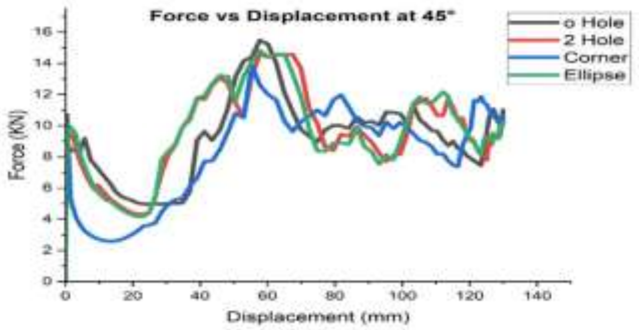

Fig -17: Force–displacement curves for all tube configurations at 45° (oblique).

7. RESULT AND DISCUSSION

This section presents numerical crashworthiness results of thin-walled aluminium square tubes with and without geometric discontinuities under axial (0deg) and oblique loading (30deg and 45deg). Four configurations are considered - intact tube and three perforated tubes with two circular holes, elliptical hole and corner holes. For the perforated cases, the area removed is kept constant at an approximate value (452-453 mm2), which allows for a constant comparison of the effect of discontinuity geometry and loading angle on the crushing response. The most important crashworthiness parameters of Peak Crushing Force (PCF), Mean Crushing Force (MCF), Energy Absorption (EA) and Specific Energy Absorption (SEA) are used to assess and compare performance.

Table -2: Result table of axial loading

Geometry	Area removed(mm2)	PCF(KN)	MCF(KN)	EA(KJ)	SEA(KJ/kg)
Without hole	0	35.96	11.75	1.528	11.575
Two holes	452.38	27.83	10.83	1.340	10.387
Elliptical hole	453.38	25.86	9.91	1.289	9.992
Corner hole	452.38	26.80	11.58	1.506	11.674

Under axial loading (Table 2), the intact tube shows the highest initial resistance and maximum absorbed energy, with PCF = 35.96 kN and EA = 1.528 kJ, reflecting an uninterrupted load path and higher axial stiffness. Introducing discontinuities significantly reduces PCF, confirming that openings act as collapse initiators by promoting earlier local yielding and folding. The two-hole and elliptical-hole configurations reduce PCF to 27.83 kN and 25.86 kN, respectively, but also reduce MCF and consequently lower EA and SEA compared with the intact tube (EA = 1.340 kJ and 1.289 kJ; SEA = 10.387 kJ/kg and 9.992 kJ/kg). In contrast, the corner-hole configuration maintains a relatively high MCF (11.58 kN) while still reducing PCF (26.80 kN), resulting in EA = 1.506 kJ and the highest SEA among axial cases (11.674 kJ/kg). This indicates that, in pure axial crushing, the corner-hole design provides a favorable balance by reducing the initial peak load while preserving progressive load-carrying capacity and overall energy absorption efficiency.

Table -3: Result table of oblique loading at 30 degrees

Geometry	Area removed(mm2)	PCF(KN)	MCF(KN)	EA(KJ)	SEA(KJ/kg)
Without hole	0	15.01	9.66	1.256	9.587
Two holes	452.38	14.92	9.79	1.273	9.868
Elliptical hole	453.38	16.67	9.80	1.275	9.883
Corner hole	452.38	14.22	8.80	1.144	8.868

At 30° oblique loading (Table 3), the force response is strongly influenced by combined compression–bending and the initial contact condition, leading to substantially lower PCF values compared with axial crushing. The intact tube records PCF = 15.01 kN and EA = 1.256 kJ. Unlike the axial case, the two-hole and elliptical-hole configurations provide slightly improved energy absorption relative to the intact tube, with

EA = 1.273 kJ and 1.275 kJ and SEA = 9.868 kJ/kg and 9.883 kJ/kg, respectively. The two-hole configuration achieves this improvement while keeping PCF essentially unchanged (14.92 kN), indicating a more stable progressive collapse without increasing the peak load. The elliptical hole attains similar EA and SEA but increases PCF to 16.67 kN, suggesting higher local resistance during collapse initiation under oblique contact, which may reduce load efficiency despite the small gain in absorbed energy. The corner-hole configuration exhibits the weakest performance at 30°, with reduced MCF (8.80 kN) and noticeably lower EA (1.144 kJ) and SEA (8.868 kJ/kg), implying that corner weakening is disadvantageous under bending-dominated crushing because it accelerates asymmetric collapse and limits the effective plastic deformation contributing to energy absorption.

Table -4: Result table of oblique loading at 45 degrees

Geometry	Area removed(mm2)	PCF(KN)	MCF(KN)	EA(KJ)	SEA(KJ/ kg)
Without hole	0	15.47	9.26	1.205	9.341
Two holes	452.38	14.59	9.63	1.253	9.713
Elliptical hole	453.38	14.81	9.65	1.255	9.728
Corner hole	452.38	14.11	8.26	1.074	8.325

At 45° oblique loading (Table 4), the bending contribution becomes more pronounced, and the intact tube shows a reduction in absorbed energy (EA = 1.205 kJ, SEA = 9.341 kJ/kg). Both the two-hole and elliptical-hole configurations outperform the intact tube, increasing EA to 1.253–1.255 kJ and SEA to 9.713–9.728 kJ/kg, while also reducing PCF relative to the intact case (14.59–14.81 kN versus 15.47 kN). This is a desirable crashworthiness outcome because it combines higher energy absorption with a lower peak load. Consistent with the 30° case, the corner-hole configuration performs worst at 45°, producing the lowest MCF (8.26 kN) and the lowest EA and SEA (1.074 kJ and 8.325 kJ/kg), indicating premature asymmetric deformation and reduced plastic work. Overall, the results demonstrate that the optimal discontinuity depends on loading direction: the corner-hole configuration is most effective in axial crushing by maintaining mean resistance and SEA, whereas the two-hole configuration provides the most consistent improvement under oblique loading by enhancing EA/SEA with favorable (or reduced) peak forces.

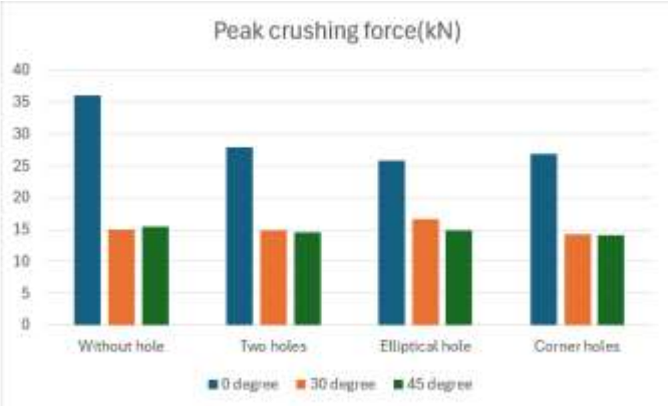

The bar charts of **peak crushing force (PCF)** and **specific energy absorption (SEA)** provide a clear comparison of the influence of discontinuity type and loading angle. As shown in the PCF chart, the **axial case (0°)** produces the largest peak loads for all geometries, with the intact tube reaching the maximum value, while introducing holes significantly reduces PCF, indicating earlier triggering of plastic collapse and reduced initial stiffness. When the loading becomes oblique (**30° and 45°**), PCF drops sharply and the differences between geometries become smaller, showing that the response is increasingly governed by bending and initial contact rather than purely axial resistance; however, the **elliptical-hole case at 30°** exhibits a comparatively higher peak than the other perforated designs, suggesting a stronger local resistance during collapse initiation under angled contact.

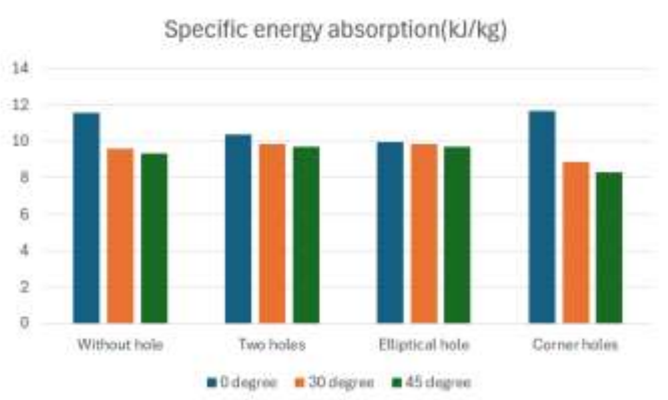

The SEA chart shows that increasing obliquity generally **reduces SEA** compared with axial loading for all configurations, reflecting the less stable progressive folding and reduced effective crushing work under bending-dominated deformation. Under **0°**, the **corner-hole configuration** provides the highest SEA, slightly exceeding the intact tube, while the two-hole and elliptical-hole designs show lower SEA. In contrast, at **30° and 45°**, the **two-hole and elliptical-hole configurations** maintain SEA values that are comparable to or slightly higher than the intact tube, whereas the **corner-hole configuration** consistently gives the lowest SEA, indicating that corner weakening is less favorable under oblique loading where asymmetric collapse becomes dominant.

8. CONCLUSIONS

This numerical study evaluated the crashworthiness of thin-walled aluminium square tubes with and without geometric discontinuities under axial (0°) and oblique (30° and 45°) crushing. With an approximately constant removed area and a fixed discontinuity location (30 mm from the top), the results show that crash response is governed primarily by **discontinuity geometry** and its interaction with **loading angle and initial contact**.

Under **axial loading**, introducing holes substantially reduced the peak load compared with the intact tube, because the discontinuities act as **collapse initiators** and reduce the initial stiffness. Among the perforated designs, the **corner-hole tube** provided the best axial efficiency (highest SEA and near-baseline EA), indicating that corner weakening promotes **stable progressive folding** while maintaining mean load capacity after the first buckle. In contrast, the **two-hole** and **elliptical-hole** tubes showed lower EA/SEA, as the removed material on the tube face encouraged **greater local softening** and reduced the sustained crushing resistance.

Under **oblique loading**, peak forces were much lower for all cases due to the dominant **compression–bending** behaviour. In this regime, the **two-hole configuration** showed the most robust performance at both 30° and 45°, achieving higher SEA than the intact tube while keeping PCF comparable or lower; this suggests the holes helped **stabilise collapse initiation** and support more consistent plastic deformation under asymmetric contact. The **elliptical hole** produced similar energy-absorption levels but showed a higher PCF at 30°, implying stronger local resistance during initial contact. The **corner-hole design** performed worst in oblique loading because removing material at the corners weakens a critical load path under bending, promoting **premature asymmetric collapse** and reduced plastic work.

Overall, the study indicates that the optimal discontinuity depends on the impact direction: **corner holes are preferable for predominantly axial energy absorbers**, whereas **two circular holes are recommended when oblique loading is expected**, as they provide the best balance between peak-load control and energy absorption across loading angles.

REFERENCES

[1] N. A. Z. Abdullah, M. S. M. Sani, M. S. Salwani, and N. A. Husain, “A review on crashworthiness studies of crash box structure,” Aug. 01, 2020, *Elsevier Ltd*. doi: 10.1016/j.tws.2020.106795.

[2] N. N. Hussain, S. P. Regalla, and Y. V. D. Rao, “Comparative Study of Trigger Configuration for Enhancement of Crashworthiness of Automobile Crash Box Subjected to Axial Impact Loading,” in *Procedia Engineering*, Elsevier Ltd, 2017, pp. 1390–1398. doi: 10.1016/j.proeng.2016.12.198.

[3] A. Dimas, T. Dirgantara, L. Gunawan, A. Jusuf, and I. S. Putra, “The effects of spot weld pitch to the axial crushing characteristics of top-hat crash box,” in *Applied Mechanics and Materials*, Trans Tech Publications Ltd, 2014, pp. 578–582. doi: 10.4028/www.scientific.net/AMM.660.578.

[4] J. Wang, Y. Zhang, N. He, and C. H. Wang, “Crashworthiness behavior of Koch fractal structures,” *Mater Des*, vol. 144, pp. 229–244, Apr. 2018, doi: 10.1016/j.matdes.2018.02.035.

[5] P. Woelke, N. Abboud, D. Tennant, E. Hansen, and C. Mcarthur, “Ship impact study: Analytical approaches and finite element modeling,” *Shock and Vibration*, vol. 19, pp. 515–525, 2012, doi: 10.3233/SAV-2011-0647.

[6] X. Xu, Y. Zhang, J. Wang, F. Jiang, and C. H. Wang, “Crashworthiness design of novel hierarchical hexagonal columns,” *Compos Struct*, vol. 194, pp. 36–48, Jun. 2018, doi: 10.1016/J.COMPSTRUCT.2018.03.099.

[7] F. Wu, T. Liu, X. Xiao, Z. Zhang, and J. Hou, “Static and dynamic crushing of novel porous crochet-sintered metal and its filled composite tube,” *Compos Struct*, vol. 209, pp. 830–843, Feb. 2019, doi: 10.1016/J.COMPSTRUCT.2018.11.022.

[8] M. S. Zahran, P. Xue, M. S. Esa, and M. M. Abdelwahab, “A novel tailor-made technique for enhancing the crashworthiness by multi-stage tubular square tubes,” *Thin-Walled Structures*, vol. 122, pp. 64–82, Jan. 2018, doi: 10.1016/J.TWS.2017.09.031.